

## ORIGINAL ARTICLE

## Bacterial magnetic particles as a novel and efficient gene vaccine delivery system

Y-S Tang, D Wang, C Zhou, W Ma, Y-Q Zhang, B Liu and S Zhang

DNA vaccination is an attractive approach for eliciting antigen-specific immunity. In this study, we used magnetosomes (bacterial magnetic particles, BMPs) as carriers of a recombinant DNA composed of a secondary lymphoid tissue chemokine, human papillomavirus type E7 (HPV-E7) and Ig-Fc fragment (pSLC-E7-Fc) to generate a gene vaccine (BMP-V) for tumour immunotherapy. The results indicate that BMPs linked to DNA more efficiently in phosphate-buffered saline (pH = 4–5) than in physiological saline. Efficient transfection of BMP-V *in vitro* and *in vivo* was achieved when a 600-mT static magnetic field was applied for 10 min. In a mouse tumour model, subcutaneous injection of BMP-V (5 µg, × 3 at 4-day intervals) plus magnetic exposure elicited systemic HPV-E7-specific immunity leading to significant tumour inhibition. The treated mice tolerated BMP-V immunisation well with no toxic side effects, as shown by histopathological examinations of major internal organs. Taken together, these results suggest that BMP can be used as a gene carrier to elicit a systemic immune response.

*Gene Therapy* (2012) 19, 1187–1195; doi:10.1038/gt.2011.197; published online 15 December 2011

**Keywords:** magnetosomes; gene delivery; vaccine; tumour

## INTRODUCTION

DNA vaccines are an attractive approach for generating antigen-specific immunity. Therefore, various delivery strategies have been investigated. The administration of DNA plasmids by conventional intramuscular injection results in suboptimal immunogenicity, even when administered at high plasmid concentrations.<sup>1</sup> The gene gun system is superior to other methods, even when administering a relatively low dose of DNA plasmid. Gene gun administration has shown potency in various animal models, including larger animals and humans.<sup>2</sup> Another promising method of DNA vaccine delivery is electroporation. However, although electroporation dramatically increases transfection efficacy, various factors influence the success of this method, including the electroporation buffer, electric pulse, pulse width, number of pulses, DNA amount and cell density. Importantly, both the gene gun and the electroporation systems require specific instruments that can be rather expensive.<sup>3</sup> At present, neither the gene gun nor the electroporation approach has become a formal clinical therapeutic method. Therefore, the identification of an effective and easy gene delivery system is critical to solving the present challenges. Recently, new bacterial magnetic nanoparticles (BMPs), called magnetosomes, have been found in magnetotactic bacteria. Magnetosomes are interesting as potential carriers of therapeutic drugs and genes for targeting cancer because of their unique features, such as paramagnetism, nanoscale size (40–120 nm) and high dispersal quality.<sup>4–9</sup> BMPs are novel nanoparticles with a presumed good biocompatibility that are covered with a stable cytoplasmic membrane; therefore, BMPs have the potential for various technological applications, allowing them to bind easily to proteins and genes.<sup>10–12</sup> Recently, a novel BMP-polyethylenimine (BMP-PEI) gene delivery system, which has a higher transfection efficiency and lower toxicity than PEI alone, has been developed.<sup>13</sup>

Our laboratory has developed a chemotactic antigen DNA vaccine system for various vaccine candidates.<sup>14</sup> One of these vaccines uses the human papillomavirus type-16 E7 (HPV-16E7) as the target antigen. The plasmid construct (pSLC-E7-Fc) contains a fused gene, in which the E7 gene is sandwiched by the secondary lymphoid tissue chemokine (SLC) and the IgG Fc fragment genes. Our previous results have illustrated that SLC and Fc can synergistically enhance the immunogenicity of an E7-expressing plasmid DNA vaccine, resulting in dramatic augmentation of systemic anti-tumour immunity against E7-expressing tumours.<sup>15</sup>

In this report, we used the tumour gene vaccine pSLC-E7-Fc to exemplify the optimised condition of BMPs as a gene carrier both *in vitro* and *in vivo*. We show the optimal conditions to form a complex in which BMPs, in association with PEI, electrostatically bind to pSLC-E7-Fc (named BMP-PEI-pSLC-E7-Fc or BMP-V in brief) and subsequently demonstrated that the complex transfected cells both *in vitro* and *in vivo*. Furthermore, we investigated the therapeutic effect of BMP-V as a DNA vaccine against E7-expressing tumours *in vivo*. We determined the optimal dose and vaccination route for BMP-V. These results demonstrate that BMPs represent a novel approach for gene delivery and provide a DNA vaccine delivery method with adequate efficacy that is also simple, inexpensive and safe.

## RESULTS

BMP–DNA complexes and efficiency of BMP linked to DNA

In previous studies, BMPs were bound to DNA in a NaCl solution. On the basis of these results, PEI, DNA and BMP were mixed in a mass ratio of 1:1:0.3.<sup>3</sup> Using the same mass ratio in phosphate-buffered saline (PBS) as with the NaCl solution, the binding efficiency of DNA to BMPs increased significantly at pH 4 and pH 5 (Figure 1). The maximum binding efficiency reached 96% in PBS,

Department of Immunology, Cancer Institute and Cancer Hospital, Peking Union Medical College and Chinese Academy of Medical Sciences, Beijing, China. Correspondence: Dr B Liu or Dr S Zhang, Department of Immunology, Cancer Institute and Cancer Hospital, Peking Union Medical College and Chinese Academy of Medical Sciences, Beijing 100021, China.

E-mail: liub11@yahoo.com or biotherapy@caca.sina.net

Received 27 May 2011; revised 26 October 2011; accepted 27 October 2011; published online 15 December 2011

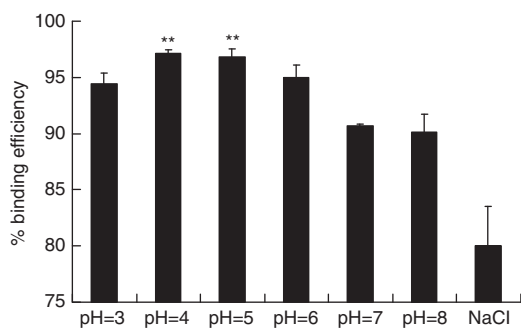


**Figure 1.** The DNA-binding efficiency of BMPs in phosphate-buffered saline at different pH values (pH = 3, 4, 5, 6, 7, 8) and 150 mM NaCl. Maximal DNA-binding efficiency was obtained at a pH of 4 and 5. \*\* $P < 0.05$  compared with the 150 mM NaCl group (pH 7).

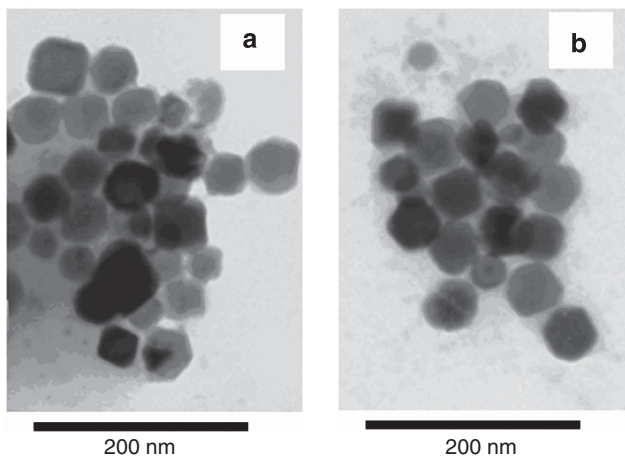


**Figure 2.** (a) Bacterial magnetic particles were obtained from *Magnetospirillum gryphiswaldense* MSR-1. The size distribution of BMPs ranged from 45 to 55 nm. (b) TEM image of BMP-V complexes. Amplification:  $\times 60\,000$ .

as compared with 79.5% in the NaCl solution ( $P < 0.05$ ). The binding efficiency in PBS at the other pH values was also slightly higher than that in the NaCl buffer. We further analysed the structures and dimensions of the BMP-V complexes by transmission electron microscopy. The complexes are homogeneous, with diameters  $< 100$  nm (Figure 2). The size and morphology of the BMP-V complexes were uniform, similar to those of un-complexed BMPs.

The effects of magnetic field and magnetofection time on transfection efficiency

To improve transfection efficiency, we altered the magnetic field strength and duration times for magnet placement under the culture plate. We used BMP-V complexes to transfect B16-F10 cells. After culturing for 48 h, we used semi-quantitative reverse transcription PCR to analyse transfection efficiency. As shown in Figure 3, the maximum transfection efficiency occurred when the magnetic field was 600 mT and the applied time was 10 min. In contrast, transfection efficiency decreased when the magnetic field was reduced to 200 mT or when the applied time was altered.

To confirm this result, we used flow cytometry to determine the outcome of transfection. Table 1 demonstrates that when a magnetic field of 600 mT was applied for 10 min, transfection efficiency peaked at 11.7%, which is not lower than that of the positive control (Lipofectamine 2000) group (9.1%). The data also

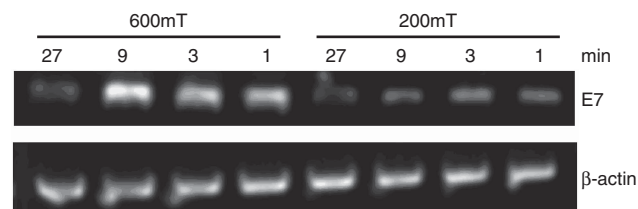


**Figure 3.** Semi-quantitative RT-PCR analysis of B16F10 cells transfected with BMP-V using various magnets and time periods. The expression was measured 48 h after transfection.

**Table 1.** Transfection efficiency of GFP

	Negative control	Positive control	600 mT			
			5 min	10 min	20 min	30 min
Transfection efficiency (%)	0.5	9.1	7.7	11.7	9.2	9.6

Abbreviations: BMP, bacterial magnetic particle; FACS, fluorescence-activated cell sorting; GFP, green fluorescent protein; pEGFP, plasmid-enhanced green fluorescent protein. B16F10 cells were transfected with BMP-GFP using various times, and GFP expression was measured by FACS 48 h after transfection. Positive control: B16F10 cells+Lipofectamine 2000/pEGFP-N1; negative control: B16F10 cells+pEGFP-N1.

show that the 600-mT magnet worked more effectively than the 200-mT magnet, but a longer exposure time did not induce higher transfection efficiency.

#### *In vivo* gene transfer of BMP-DNA complexes

Administration of a luciferase DNA plasmid and subsequent luminescent imaging has been verified to quantitatively evaluate the efficacy of gene transfer.<sup>16</sup> After optimal conditions for transfecting BMPs-DNA complexes *in vitro* were determined, their ability to transduce tissues was further elucidated *in vivo*. BMPs mixed with pGL4.17 were administered to C57BL/6 mice through subcutaneous (s.c.) injection with or without the application of a 600-mT magnet on the injection site for 10 min. The results show that the expression of a luciferase reporter was clearly observed in the tissue injected with BMPs-pGL4.17 with the magnet as compared with those without the magnet (Figure 4). Therefore, BMP-based delivery of the gene vaccine into the cells is simple, and the combination of BMPs and the magnet is crucial for successful *in vivo* transfection.

S.c. injection with magnet application resulted in an increased tumour inhibition as compared with other methods of BMP-V administration

Mice were challenged with TC-1 tumour cells intravenously followed by vaccination with BMP-V, which was administered using various methods. In brief, C57BL/6 mice were vaccinated with 20  $\mu$ g BMP-V through intramuscular injection or s.c. injection with or without magnet application. Figure 5 demonstrates that vaccination by s.c. injection with the magnet systemically inhibited the growth of metastatic lung tumours, as quantified by scoring of the total lung weight of mice. The average weight of the lungs of mice treated with PBS was  $642.02 \pm 71.873$  mg. This weight was significantly different from the lung weight of BMP-V-treated mice ( $296.56 \pm 64.209$  mg;  $P < 0.05$ ). The mean number of lung tumour nodules in mice vaccinated with a s.c. injection of BMP-V plus magnet ( $42.6 \pm 8.28387$ ) was considerably lower than

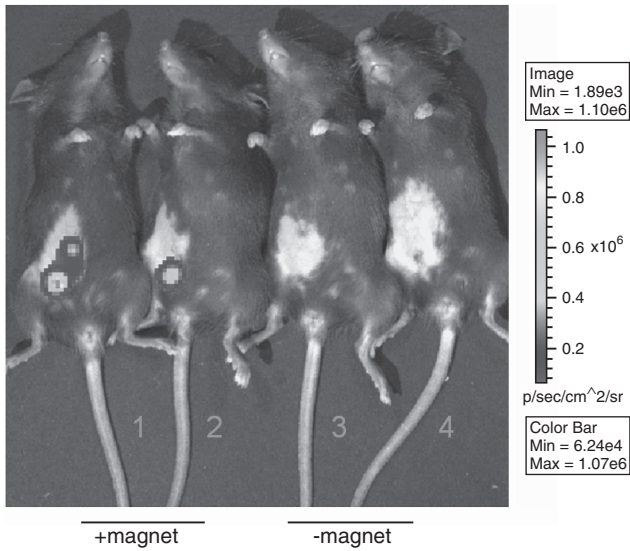


**Figure 4.** Luciferase gene delivery by BMPs-pGL4.17 with or without a magnet. C57BL/6 mice were vaccinated with 10  $\mu$ g BMPs-pGL4.17 by subcutaneous injection with a magnet on the injection site for 10 min (1, 2) or without a magnet (3, 4). Luciferase imaging was performed at 48 h after vaccination.

that in mice vaccinated with PBS ( $194.8 \pm 23.64849$ ;  $P < 0.05$ ). Intramuscular vaccination with BMP-V had a slight effect, but did not demonstrate a statistically significant difference from that of the PBS group.

Vaccination of mice with a low dose of BMP-V induces a strong tumour-specific immune response

Next, the therapeutic effects of different doses of BMP-V in the s.c. TC-1 tumour model were compared. As shown in Figure 6a, 5–40  $\mu$ g BMP-V immunotherapy suppressed tumour growth and clearly lengthened the lifetime of tumour-bearing mice (Figure 6b) as compared with the PBS control. However, the therapeutic effects between the BMP-V treatment groups did not demonstrate significant differences. Therefore, a 5- $\mu$ g dosage is sufficient for treatment.

Vaccination of mice with BMP-V, followed by a 10-min magnet application inhibits the growth of experimental metastases

We next examined the effects of different lengths of magnet application to facilitate BMP-V delivery. Using the TC-1 lung metastasis model, we demonstrated that 10 min is the optimal magnetofection time for the BMP-V-mediated tumour therapeutic effect. As shown in Figure 7a, the average pulmonary metastatic tumour weight (grams) of mice treated with PBS was  $343.6 \pm 44.9$  mg, which was significantly higher than that in mice vaccinated with BMP-V with the magnet placed on the surface of the injection site for 10 min ( $58.9 \pm 9.5$  mg;  $P < 0.05$ ). Similar results were obtained for the mean number of lung tumour nodules ( $135 \pm 28$  vs  $53 \pm 12$ ;  $P < 0.05$ , Figure 7b).

BMP-V administration generates an E7-specific CD8 + T

As shown in Figure 8, splenocytes from mice treated with 5  $\mu$ g BMP-V resulted in higher cytotoxic T lymphocyte activities ( $26.20 \pm 3.96\%$  at E:T = 60:1) compared with those from mice immunised with PBS ( $2.32 \pm 0.15\%$  at E:T = 60:1) when TC-1 cells were used as target cells. The specificity of killing was demonstrated by the inability of the splenocytes of BMP-V-vaccinated mice to kill B16-F10 cells that expressed irrelevant antigens. These data demonstrate that BMP-V can induce antigen-specific cytotoxic T lymphocyte activity.

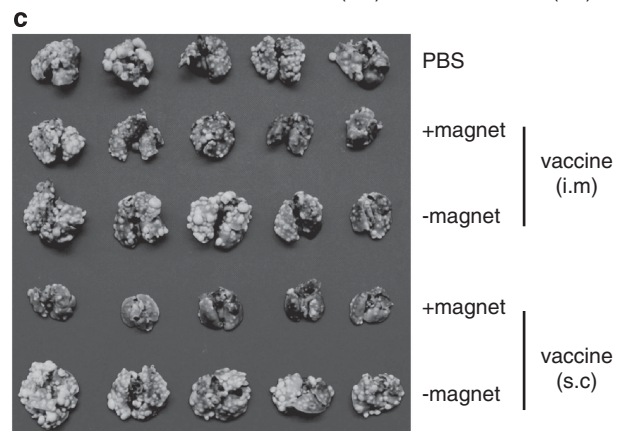
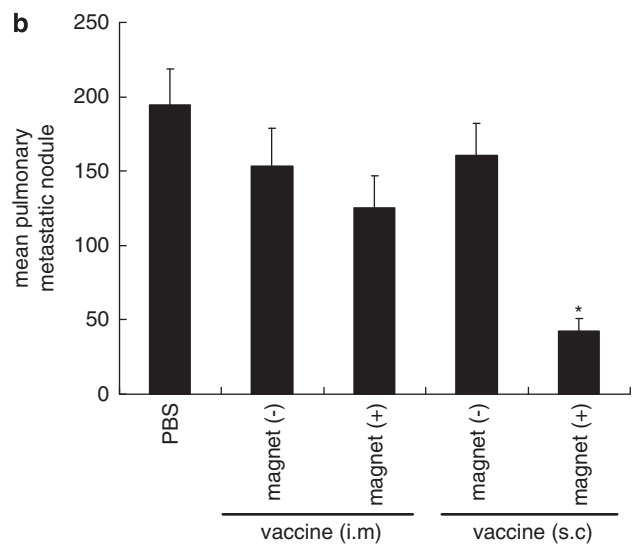
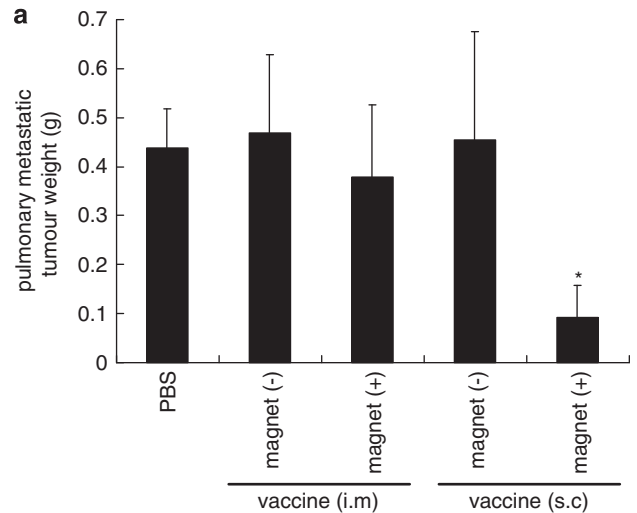


**Figure 5.** Pulmonary tumour nodules and pulmonary metastatic tumour weight in mice vaccinated with BMP-V vaccine through various routes of administration. Mice ( $n = 5$ ) were challenged with TC-1 cells through the tail vein. On day 4, mice were randomised and treated with 20  $\mu$ g BMP-V in 0.1 ml PBS or PBS alone. The same treatments were repeated on days 8 and 12. All of the mice were killed on day 25. (a) Pulmonary metastatic tumour weights were measured.  $*P < 0.05$  compared with the PBS group. (b) Data are presented as the mean number of pulmonary tumour nodules  $\pm$  s.d. of five mice per group in a representative experiment.  $*$ Indicates  $P < 0.05$  compared with the PBS group. (c) Gross picture of pulmonary tumours in each vaccinated group. Experiments were repeated in duplicate with similar results.

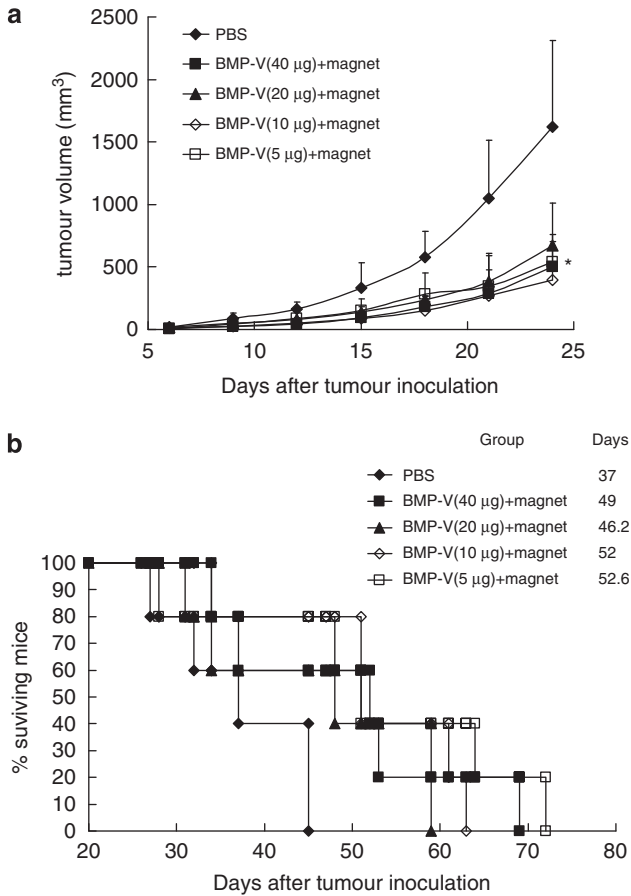


**Figure 6.** The anti-tumour effects of different amounts of BMP-V. C57BL/6 mice inoculated s.c. with  $5 \times 10^4$  TC-1 cells. When tumours reached an average diameter of  $\sim 5$  mm on day 4, mice were randomised and treated with different doses of BMP-V (40, 20, 10, 5  $\mu$ g of BMP-V in 0.1 ml PBS or PBS alone). The same treatments were repeated on days 8 and 12. BMP-V were delivered to mice in the shaved inguinal region through subcutaneous injection with a magnet (magnetic flux density of 600 mT) on the injection site for 10 min. **(a)** Tumour volumes were monitored for 25 days until the control mice began to die. Data are presented as mean tumour volumes  $\pm$  s.d. of five mice per group in a representative experiment. \*Indicates  $P < 0.05$ , all treatments compared with PBS. **(b)** Survival of mice per treatment group. The results of both experiments were pooled in a stratified analysis, resulting in  $P > 0.05$  when the 5  $\mu$ g BMP-V-treated group was compared with the 10  $\mu$ g BMP-V-treated group and  $P < 0.05$  when the 5  $\mu$ g BMP-V-treated group was compared with the PBS group. Data are representative of three independent experiments. MST: mean survival time.

#### Significant tumour-infiltrating lymphocytes (TILs) in tumours of mice vaccinated with BMP-V

Previous studies have suggested that the presence of a substantial number of TILs dramatically affects the clinical prognosis of patients. Patients with increased TILs live longer than do those whose tumours lack a large number of TILs.<sup>17</sup> In this study, we determined whether TILs were detectable in mice treated with BMP-V. As shown in Figure 9, tumours of mice vaccinated with BMP-V carried a significant number of TILs, whereas tumours of mice vaccinated with PBS had relatively fewer TILs.

Vaccination of mice with BMP-V is non-toxic to the main organs. Bacterial magnetic particles are of great interest as potential carriers of bioactive materials, drugs and genes because of their

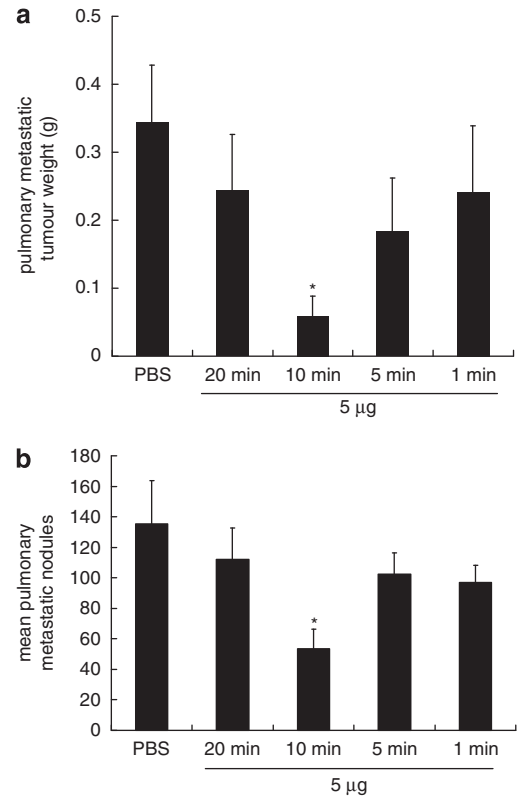


**Figure 7.** Pulmonary tumour nodules and pulmonary metastatic tumour weights in mice vaccinated with BMP-V using various times. Mice ( $n = 5$ ) were challenged with TC-1 cells through the tail vein. On day 4, mice were randomised and treated with 5  $\mu$ g of BMP-V in 0.1 ml of PBS or PBS alone. The same treatments were repeated on days 8 and 12. BMP-V was administered to mice in the shaved inguinal region through subcutaneous injection with a magnet (magnetic flux density of 600 mT) on the injection site for various times (1, 5, 10, 20 min). All of the mice were killed on day 25. **(a)** Pulmonary metastatic tumour weights were measured. \* $P < 0.05$  compared with the PBS group. **(b)** Data are presented as the mean number of pulmonary tumour nodules  $\pm$  s.d. of five mice per group in a representative experiment. \*Indicates  $P < 0.05$  compared with the PBS group.

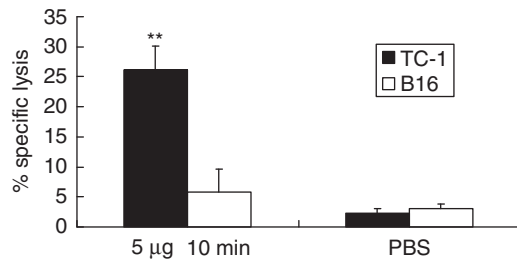


**Figure 8.** CTL responses in mice ( $n = 3$ ) immunised with 5  $\mu$ g of BMP-V plus magnet for 10 min or PBS on days 4, 8 and 12 after TC-1 cell challenge (day 0). On day 18, pooled spleen cells were harvested, and a standard LDH assay was performed. Effector cells from each group were harvested and cytotoxicity was tested against B16 and TC-1 tumour cells at an E:T ratio of 60:1. Data are presented as mean percentage specific lysis  $\pm$  s.d. of triplicate wells of a pooled sample per group in a representative experiment. Experiments were repeated in triplicate with similar results. \*\*Indicates  $P < 0.05$ , compared with the no-treatment group.

nano-scale size and lipid membrane. We determined whether BMPs were toxic to the body when used as gene carriers. Histological examination (Figure 10) of the heart, liver, kidney,



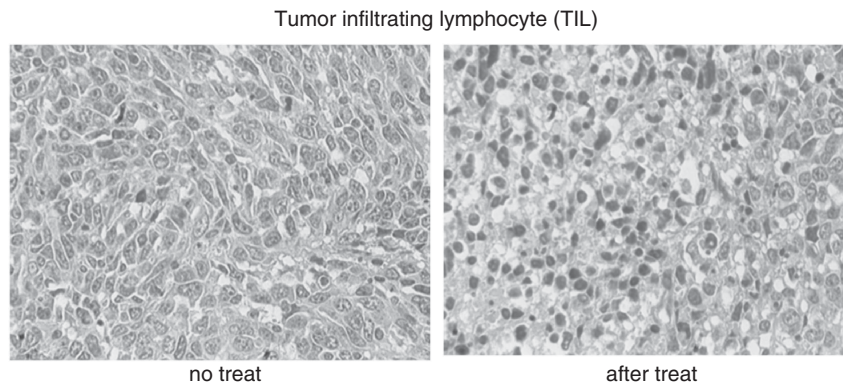


**Figure 9.** Here,  $5 \times 10^4$  TC-1 cells were inoculated in the right flank of C57BL/6 mice ( $n = 3$ ) s.c. (day 0). On day 4, mice were randomised and treated with  $5 \mu\text{g}$  BMP-V in 0.1 ml of PBS or PBS alone. The same treatments were repeated on days 8 and 12. BMP-V was administered to mice in the shaved inguinal region through subcutaneous injection with a magnet (magnetic flux density of 600 mT) on the injection site for 10 min. Tumours were excised 3 days after the third vaccination. We performed HE staining of TIL from C57BL/6 mice in the PBS group (left) and the BMP-V treatment group (right). Images are representative of multiple microscopic fields observed in at least three mice per group.

spleen and lung indicated that there was no significant difference between the BMP-V-treated and normal mouse groups.

#### BMPs lack immunogenicity

In this study, we investigated the effect of BMPs on BMP-V efficacy when administered s.c. To evaluate the immunogenicity of BMPs, mice were immunised with different doses of BMPs. Blood was collected after two immunisations. As shown in Figure 11, mice vaccinated with 5 or  $20 \mu\text{g}$  of BMPs lacked the anti-BMPs antibody. The results were not significantly different from those for mice vaccinated with PBS.

## DISCUSSION

Bacterial magnetic particles have drawn a great deal of attention since 1975; previous research has focused primarily on their mechanism of biosynthesis.<sup>18,19</sup> Importantly, Hopkin<sup>20</sup> predicted that BMPs could be used as vectors of drugs for targeted tumour therapy. However, applying BMPs as a gene delivery system in animals is still relatively rare.

A previous study has demonstrated the formation of BMPs-PEI-DNA complexes in NaCl.<sup>13</sup> In this report, we have demonstrated that the binding efficiency is considerably higher when BMPs complexes bind DNA in PBS at pH levels of 4 and 5 than in 150 mM NaCl. The negative charges of DNA interact with positive charges of acidic PBS, which may cause the DNA to bind to BMP complexes more efficiently. Hergt *et al.*<sup>21</sup> have demonstrated the magnetic properties of BMPs as potential diagnostic and therapeutic tools. In this report, we determined that a magnetic field of 600 mT and an incubation time of 10 min are optimal for gene transfer using BMPs-DNA complexes (Figure 3 and Table 1). In general, B16 melanoma cells are difficult to transfect. The transfection efficiency of Lipofectamine 2000 was 9.1%, whereas that of BMPs-DNA complexes (600 mT, 10 min) was 11.7%. The use of a 600-mT static magnetic field can achieve a higher transfection rate than the use of a 200-mT field *in vitro* (Figure 3). In addition, the application of a magnetic field *in vivo* greatly improved transfection efficiency (Figure 4). These results demonstrate that BMPs, with the help of a magnetic force, may accelerate the accumulation of complexes on the surface of cells and that the contribution of the magnetic force can enhance nuclear uptake of magnetic particles in the process of magnetofection. Under an increased magnetic force, BMP-DNA complexes may reach the surface of the cells more quickly and may promote the entry of plasmid DNA into the cells more efficiently.

On the basis of the *in vivo* experiments, we demonstrated that a BMP-carrier gene vaccine plus a magnetic field results in tumour protection. Few studies have demonstrated DNA expression using BMPs in an animal model. Xiang *et al.*<sup>13</sup> have demonstrated that BMPs-PEI-DNA complexes induce antibody production and T-cell proliferation. Han *et al.*<sup>22</sup> investigated the therapeutic effect of small-interfering RNA-modified BMPs by injecting them into a s.c. tumour. However, this study used only the small size and favourable dispersion characteristics of BMPs, whereas we used the BMPs as a gene delivery vector and the paramagnetism of BMPs. With the application of a magnetic field, we demonstrated that the delivery of the BMP-carrier gene vaccine in normal tissue (not in tumoural tissue) generates a specific anti-tumour immune response against both s.c. and metastatic tumours.

We compared two injection methods (intramuscular vs s.c.) for BMP-V vaccination and illustrated that s.c. injection with magnet application resulted in an increased tumour protection as compared with intramuscular injection. BMPs carry the gene vaccine (pSLC-E7-Fc) into skin cells, wherein the SLC-E7-Fc fusion protein is subsequently expressed and secreted.<sup>23</sup> The secreted SLC-E7-Fc can recruit a large number of dendritic cells, especially Langerhans cells, at the vaccination site, which may facilitate antigen presentation.<sup>24-27</sup> Regardless of the effect of the gene vaccine pSLC-E7-Fc, the delivery method (s.c. plus a magnetic field) itself may target intradermal Langerhans cells and other professional antigen-presenting cells, which can prime antigen-specific T cells. This advantage is similar to the gene gun system.<sup>28,29</sup>

For conventional intramuscular injection, previous studies have often required  $50 \mu\text{g}$  of DNA to generate robust numbers of CD8+ cells in mouse models.<sup>30</sup> Therefore, we determined the optimal dose when administering BMP-V in the tumour model. The results demonstrate that vaccination of mice with as little as  $5 \mu\text{g}$  of BMP-V induces strong protection against E7+ tumours and exhibited no significant difference from the other dose groups ( $10, 20$  and  $40 \mu\text{g}$ ). Therefore, the dosage of our new vaccination method is much lower than the dosage used for conventional intramuscular injection.

Similar to the *in vitro* results, vaccination of mice with BMP-V with the magnet placed on the surface of the injection site for 10 min can inhibit the growth of tumours. The 600-mT field for 10 min adopted herein induced increased tumour inhibition as compared with other exposure times. In a shorter time under a static magnetic field, the BMP-V cannot enter the cell effectively; but a longer exposure time (27 min, Figure 3; 20 min, Figure 7) destroys the gene vaccine because the BMP-V passes through the

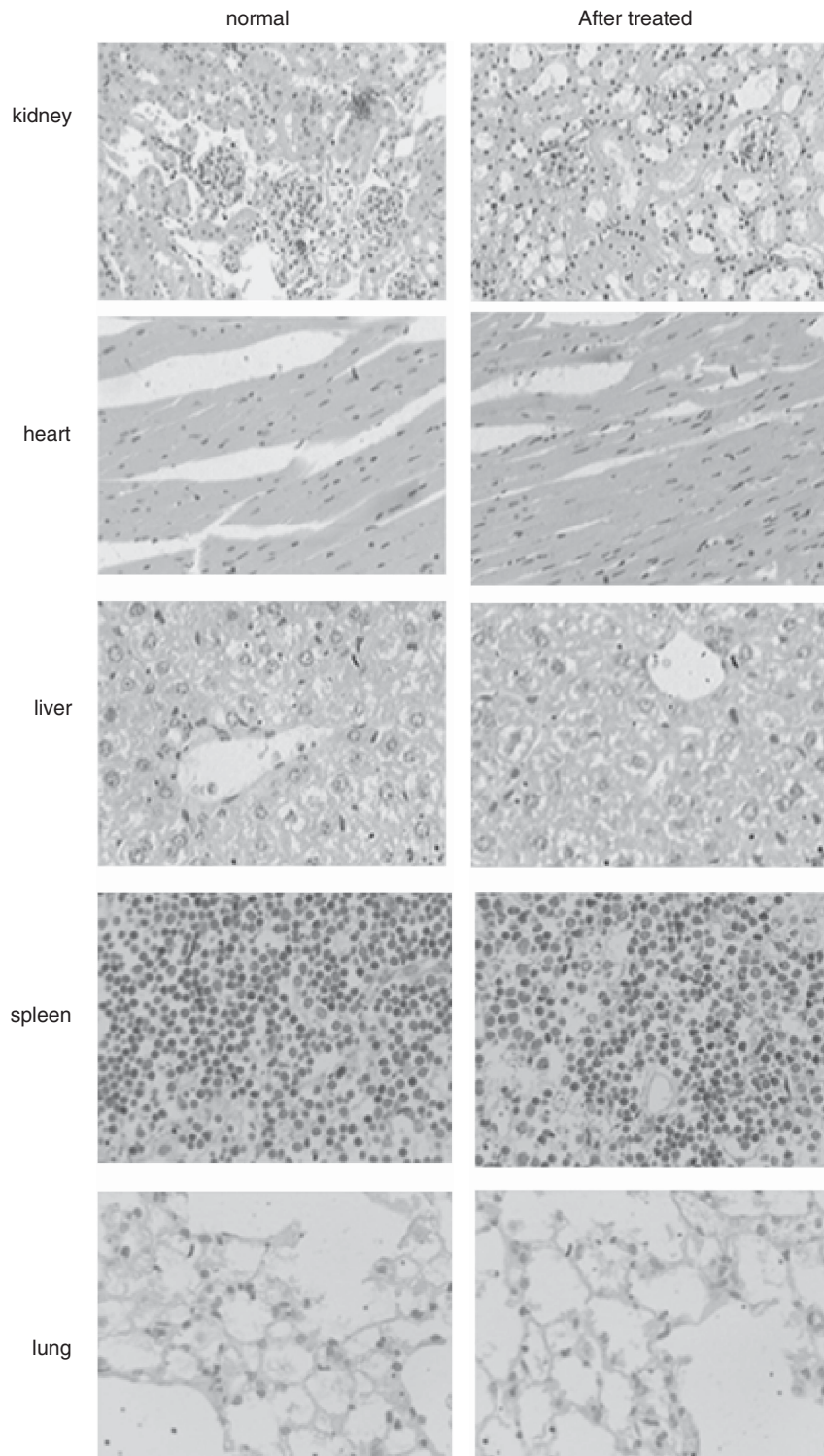


**Figure 10.** C57BL/6 ( $n = 3$ ) mice inoculated s.c. with  $5 \times 10^4$  TC-1 cells. On day 4, mice were randomised and treated with  $5 \mu\text{g}$  BMP-V in 0.1 ml PBS. The same treatments were repeated on days 8 and 12. BMP-V was administered to mice in the shaved inguinal region through subcutaneous injection with a magnet (magnetic flux density of 600 mT) on the injection site for 10 min. All of the mice were killed on day 25. We performed HE staining of the kidney, heart, liver, spleen and lung from C57BL/6 mice; normal mice (left), mice treated with BMP-V (right).

cell membrane repeatedly. Moreover, in magnetofection, cellular responses induced during the process varied and depended on many factors, including the intensity and frequency of the magnetic field, the waveform and the type of cells used.<sup>31</sup> Various magnetic forces and exposure times induce different changes in

cell shape, surface and cytoskeleton.<sup>32-36</sup> Recently, Smith *et al.*<sup>37</sup> have demonstrated that the magnetic field causes many changes in cellular gene expression in cells. Their results illustrate that magnetic static fields and exposure time should be modelled and analysed before application in culture as cells clearly respond

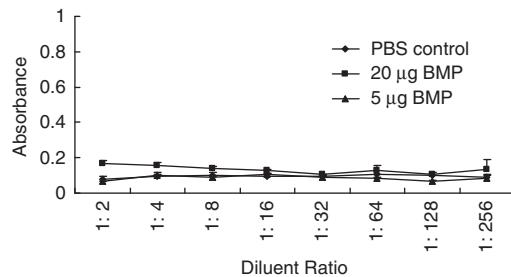


**Figure 11.** BMPs lack immunogenicity. BMPs (20 or 5 µg) were delivered to mice ( $n = 3$ ) in the shaved inguinal region through subcutaneous injection with a magnet (magnetic flux density of 600 mT) on the injection site for 10 min and then were boosted 22 days later. As a negative control, mice were treated with PBS. Seven days after the booster, blood was individually collected from the orbital vein, and the serum was prepared. The serum level of anti-BMP antibodies was determined by ELISA.

differently.<sup>37</sup> However, the mechanism regarding the effects of magnetic field in magnetofection are still unknown and require extensive research for further validation. Herein, we have determined the optimal intensity of magnetic fields and exposure time when BMPs are applied as gene carriers *in vitro* and *in vivo*.

Compared with the PBS control, BMP-carrier gene vaccine administration generates greater levels of the E7-specific cytotoxic CD8<sup>+</sup> T. Tumours of mice vaccinated with BMP-V had significant concentrations of TILs. As BMPs lack immunogenicity (Figure 11), the immune response induced by BMP-V administration is E7-specific only.

In addition, we also found that vaccination of mice with BMP-V is not toxic to the kidney, heart, liver, spleen or lung. Histological examination of these organs showed no obvious pathological changes. These data are consistent with the observations of Sun *et al.*<sup>38</sup>

Gene therapy and DNA vaccine technologies have motivated the search for the most efficient methods of gene delivery *in vivo*. BMPs are synthesised in the organism and cause no toxicity to cells. The cytoplasmic membrane of BMPs provides a presumed good biocompatibility *in vivo*. In this study, we preliminarily illustrated the optimised conditions of BMPs as gene delivery systems *in vitro* and *in vivo*. Importantly, we demonstrated that the BMP vaccine system elicits systemic antigen-specific immunity. To our knowledge, this study is the first to demonstrate the effect of tumour gene vaccine delivery by BMPs in an animal model. We conclude that BMPs could be a promising vehicle for DNA delivery in gene vaccinations.

## MATERIALS AND METHODS

### Cell lines

C57BL/6 melanoma B16-F10 and Lewis's lung carcinoma cell lines were kindly provided by L Chen (Department of Immunology, Mayo Graduate and Medical Schools, Mayo Clinic, Rochester, MN, USA) and were cultured in RPMI 1640 medium (Gibco-BRL, Carlsbad, CA, USA) supplemented with 10% fetal calf serum (heat-inactivated). Mouse TC-1 tumour cells, derived from primary epithelial cells of C57BL/6 mice co-transformed with HPV-16 E6 and E7 and c-Ha-Ras oncogene, were a kind gift from Dr TC Wu (Johns Hopkins Medical Institutions, Baltimore, MD, USA) and were cultured in RPMI 1640 medium (Gibco-BRL) supplemented with 10% fetal calf serum (heat-inactivated) and 400 µg/ml G418.

### Mice

Inbred female C57BL/6 mice (6–8 weeks of age) were purchased from the Animal Centre of Chinese Academy of Medical Sciences (Beijing, China) and housed under specific pathogen-free conditions.

### Plasmids

The luciferase reporter vector pGL4.17 (luc2/Neo) (Promega, Madison, WI, USA) and luciferin substrate (Promega) were kindly provided by Professor Chen Lin (State Key Laboratory of Molecular Oncology, Cancer Institute, Peking Union Medical College and Chinese Academy of Medical Sciences). pEGFP-N1, encoding the green fluorescent protein, was purchased from Invitrogen (Carlsbad, CA, USA).

### PEI and BMP

BMPs, which were produced by the bacterium *Magnetospirillum gryphiswaldense* MSR-1 and PEI (25 kDa from Aldrich, St Louis, MO, USA; 10 mg ml<sup>-1</sup>, pH 7.2) were kindly provided by Professor Ying Li (Microbiology Department, College of Biological Sciences, China Agricultural University). PEI was diluted with deionised water to a working concentration of 2 mg ml<sup>-1</sup>. All BMPs were sterilised by γ-rays (15 kGy).

### DNA-binding assay

The polyplexes of DNA, PEI and BMPs were prepared at mass ratios of DNA:PEI:BMP = 1:1:0.3. These polyplexes were formed in PBS (8 g NaCl, 0.2 g KCl, 2.87 g Na<sub>2</sub>HPO<sub>4</sub> · 12H<sub>2</sub>O and 0.2 g KH<sub>2</sub>PO<sub>4</sub> diluted in 1000 ml of water) at different pH values and in 150 mM NaCl. The DNA concentration was determined using ultraviolet photometry both before and after the binding reaction with BMPs. The linkage rate was calculated using the following equation: Linkage rate (DNA mg/BMPs mg) =  $(C1 \times V1 - C2 \times V2)/M$ . C1 is the concentration of DNA before the binding reaction with BMPs; C2 is the concentration of DNA after the binding reaction with BMPs; V1 is the volume of the DNA solution before the binding reaction with BMPs; V2 is the volume of the DNA solution after the binding reaction with BMPs; and M is the weight of BMPs conjugated with DNA. The DNA was quantified using spectrophotometry at OD280.

### Electron microscopy

Purified BMPs were resuspended in 20 µl PBS and placed onto carbon-coated copper grids. Samples were viewed and recorded using a Philips Tecnai F30 transmission electron microscope (Philips, Holland, MI, USA) at an accelerating voltage of 300 kV.

For electron micrograph visualisation, 1 µl of plasmid DNA at 2 µg µl<sup>-1</sup> was mixed with 0.6 µg of BMPs and 2 µg of PEI in PBS at a pH = 4–5. Next, 20 µl of BMP-PEI-DNA complexes were applied to the copper grid covered with Formvar support, which had been briefly treated in a sputter coater. The grids were negatively stained for 10 min with 1% uranyl acetate. Electron micrographs were obtained on an electron microscope operating at × 60 000 magnification.

### Cell transfection

To determine the optimal pH of the PBS, the BMP-V complexes were prepared at mass ratios of DNA:PEI:BMP = 1:1:0.3 in PBS at pH = 4–5. B16-F10 cells were seeded in 24-well plates at a density of  $2 \times 10^4$  cells per well and cultured for 12 h before transfection. Cells were transfected with 5 µg of BMPs-pEGFP-N1 (BMP-GFP) per well or 5 µg of BMPs-pSLC-E7-Fc (BMP-V) per well. After the complexes were added to cells, two separate magnet densities were used to force the complexes to enter the cells within four separate time frames. A neodymium-iron-boron (Nd-Fe-B) permanent magnet, which led to a magnetic flux density of either 200 or 600 mT, was placed under the culture plates separately for 1, 3, 9 or 27 min. pEGFP-N1 complexed with Lipofectamine 2000 (Invitrogen) was used as a positive control, and transfection was performed according to the manufacturer's protocol. All cells were cultured in an incubator (37 °C with 5% CO<sub>2</sub>) for 48 h.

### Semi-quantitative reverse-transcription PCR

After incubation for 48 h, cells transfected with BMP-V were harvested and washed with PBS. Total RNA was then extracted using Trizol reagent (Invitrogen) and quantified by spectrophotometry at OD260. First-strand cDNA was synthesised using Oligo(dT)12–18 primers (Invitrogen) and SuperScript II RNase H Reverse Transcriptase (Invitrogen) according to the



manufacturer's recommendations. The target cDNA was amplified using Platinum Taq DNA Polymerase (Invitrogen) for 28–30 cycles. PCR was performed with the following primers: P1 and P2 for E7, P3 and P4 for  $\beta$ -actin (P1:5'-CGAATTCATGCACGGAGATACACC-3', P2:5'-TGATATCTGGTTT CCGAGAACAG-3', P3:5'-TTGTTACCAACTGGGACGACATGG-3' and P4:5'-GAT CTTGATCTTCATGGTCTAGG-3'). Each sample was then analysed by electrophoresis, and the resulting gel was photographed using a UVP gel documentation system (UVP, Upland, CA, USA).

#### Flow cytometry

After incubation for 48 h, cells transfected with BMP-GFP were collected and washed with PBS. The samples were fixed with PBS containing 1% paraformaldehyde and analysed by flow cytometry (Beckman Coulter, Fullerton, CA, USA).

#### Luciferase expression

The BMPs-pGL4.17 complexes were prepared at mass ratios of pGL4.17:PEI:BMP = 1:1:0.3 in PBS at pH = 4–5. In all, 10  $\mu$ g of BMPs-pGL4.17 were delivered to the shaved mouse inguinal region s.c., and a magnet was applied to the injection site for 10 min. As a control, mice received an injection of BMPs-pGL4.17 s.c. without the magnet. Forty-eight hours after vaccination, 200  $\mu$ l of luciferin diluted in PBS (15 mg ml<sup>-1</sup>) was injected intraperitoneally. After 10 min, mice were anaesthetised with chloral hydrate, and optical imaging was performed using a CCD camera and black box at the Small Animal Imaging Resource Program (Lumina Imaging System, IVIS, Caliper, Newton, MA, USA). The duration of luminescence acquisition was 120 s. The maximal level of luminescence was acquired from a region of interest drawn over the luminescent zone on the optical image.

#### Cytotoxicity assays

Female C57BL/6 mice ( $n = 3$ ) were challenged s.c. with  $5 \times 10^4$  TC-1 cells per mouse in the right flank. Four days later, mice were divided into a control group and an immunisation group, in which they were given PBS or 5  $\mu$ g BMP-V s.c. plus magnet, respectively. Mice were boosted twice with a similar regimen on days 8 and 12. Six days after the final booster, splenocytes from immunised and control mice were used as effector cells. B16-F10, Lewis's lung carcinoma and YAC-1 cells were used as target cells. Effector cells were added to target cells at a ratio of 60:1, 30:1 and 15:1 (tested in triplicate). After incubation for 4 h, the supernatants were pooled and measured for the release of lactate dehydrogenase using a CytoTox 96 Non-Radioactive Cytotoxicity Assay kit (Promega) according to the manufacturer's instructions. Specific lysis was calculated according to the following formula: cytotoxicity (%) =  $\frac{([E - Se - St])}{([Mt - St])} \times 100$ , where E is the experimental lactate dehydrogenase release in effector plus target cell co-cultures, Se is the spontaneous release by effector cells alone, St is the spontaneous release by target cells alone, and Mt is the maximal release by target cells.

#### Tumour models and treatment protocol

For the *in vivo* therapeutic experiment,  $5 \times 10^4$  TC-1 cells were inoculated s.c. into the right flank of C57BL/6 mice on day 0. When the tumour reached an average diameter of  $\sim 5$  mm on day 4, mice were randomised and treated with different doses of BMP-V in 0.1 ml of PBS or PBS alone. Similar treatments were repeated on days 8 and 12. BMP-V was delivered to the shaved inguinal region of the mice through s.c. injection with or without a magnet (magnetic flux density of 600 mT) on the injection site for 10 min. Tumours were monitored every 3 days by measuring their dimensions using callipers and calculating their volumes according to the following formula: tumour volume (mm<sup>3</sup>) =  $0.52 \times (\text{length} \times \text{width}^2)$ .

For the TC-1 experimental pulmonary metastasis model, mice (five mice per group) were challenged with  $1 \times 10^5$  TC-1 cells per mouse through the tail vein on day 0. On day 4, mice were randomised and treated with different doses of BMP-V in 0.1 ml of PBS or PBS alone. Similar treatments were repeated on days 8 and 12. BMP-V was administered to mice either intramuscularly to the leg or s.c. to the shaved inguinal region with or

without a magnet (magnetic flux density of 600 mT) on the injection site for different time periods. All of the mice were killed on day 25, and the resected lungs were weighed and fixed in Bouin's solution (picric acid saturated aqueous solution:formalin:glacial acetic acid = 15:5:1) for 24 h. After fixation, the lungs became yellow and the tumour nodules turned white, allowing the number of pulmonary metastatic nodules to be counted using a magnifier by blinded researchers.

#### Histology

TC-1-bearing mice were treated according to the BMP-V treatment protocol described earlier. Tumours were excised 3 days after the third vaccination. The hearts, kidneys, livers, spleens and lungs of each mouse were excised 13 days after the third vaccination. The organs were fixed for 24 h in 10% neutral-buffered formalin, embedded in paraffin and sectioned. The sections were stained with hematoxylin-eosin. Hematoxylin-eosin sections were observed ( $\times 400$ ) by several professional pathologists.

#### Serum collection and BMP immunogenicity measurements

BMPs (5 or 20  $\mu$ g) were delivered to mice ( $n = 3$ ) in the shaved inguinal region through s.c. injection and treated with a magnet (magnetic flux density of 600 mT) on the injection site for 10 min, and a similar procedure was repeated on day 22. As a negative control, mice were injected with PBS. Seven days after the booster, blood samples collected from each group through the orbital vein were poured into separate glass tubes, clotted, chilled to 4 °C and centrifuged for 20 min at 3000 r.p.m. Serum was collected and diluted with 0.05% Tween-20 and 10% fetal bovine serum in PBS. In all, 20  $\mu$ g BMP was used to coat 96-well plates. After adding the diluted serum samples in triplicate, plates were incubated for 2 h and washed three times with 0.05% Tween-20 and 10% fetal bovine serum in PBS. After three washes, the plates were then incubated with 50 ng ml<sup>-1</sup> biotinylated goat anti-mouse IgG (R&D Systems, Minneapolis, MN, USA) for 2 h. After three additional washes, the plates were incubated with streptavidin conjugated to horseradish peroxidase for 20 min. The plates were then washed again and incubated with substrates for 20 min. The reactions were stopped with 2 N H<sub>2</sub>SO<sub>4</sub> (R&D Systems), and the plates were read at 450 nm with a correction wavelength of 570 nm.

#### Statistical analysis

To compare individual time points, analysis of variance was used for comparisons among three or more groups. Student's *t*-test was used to compare the means between the two groups. Survival data from the animal studies were analysed using the log-rank test. Differences were considered to be significant when  $P < 0.05$ . Statistical analysis was performed using commercially available software (SPSS 11.0, SPSS, Chicago, IL, USA).

#### CONFLICT OF INTEREST

The authors declare no conflict of interest.

#### ACKNOWLEDGEMENTS

We thank Professor Y Li (China Agricultural University) for magnetosomes and Yongquan Wang and Zheng Wang for their excellent work with the animal experiments. This work was supported by a grant from the 863 High-Tech Projects of the Chinese Government (No. 2007AA021805).

#### REFERENCES

- Bansal A, Jackson B, West K, Wang S, Lu S, Kennedy JS *et al*. Multifunctional T-cell characteristics induced by a polyvalent DNA prime/protein boost human immunodeficiency virus type 1 vaccine regimen given to healthy adults are dependent on the route and dose of administration. *J Virol* 2008; **8**: 6458–6469.
- Donnelly J, Berry K, Ulmer JB. Technical and regulatory hurdles for DNA vaccines. *Int J Parasitol* 2003; **33**: 457–467.
- Nicolas JF, Guy B. Intradermal, epidermal and transcutaneous vaccination: from immunology to clinical practice. *Expert Rev Vaccines* 2008; **7**: 1201–1214.
- Bazyliński DA, Frankel RB. Magnetosome formation in prokaryotes. *Nat Rev Microbiol* 2004; **2**: 217–230.



- 5 Bazylinski DA, Garratt-Reed AR, Frankel B. Electron-microscopic studies of magnetosomes in magnetotactic bacteria. *Microsc Res Techniq* 1994; **27**: 389-401.
- 6 Hoell A, Wiedenmann A, Heyen U, Schüler D. Nanostructure and field-induced arrangement of magnetosomes studied by SANSPO. *Physica B* 2004; **350**: 309-313.
- 7 Lang C, Schüler D, Favre D. Synthesis of magnetite nanoparticles for bio- and nanotechnology: genetic engineering and biomimetics of bacterial magnetosomes. *Macromol Biosci* 2007; **7**: 144-151.
- 8 Matsunaga T, Suzuki T, Tanaka M, Arakaki A. Molecular analysis of magnetotactic bacteria and development of functional bacterial magnetic particles for nanobiotechnology. *Trends Biotechnol* 2007; **25**: 182-188.
- 9 Favre D, Schüler D. Magnetotactic bacteria and magnetosomes. *Chem Rev* 2008; **108**: 4875-4898.
- 10 Xie J, Chen K, Chen X. Production, modification and bio-applications of magnetic nanoparticles gestated by magnetotactic bacteria. *Nano Res* 2009; **2**: 261-278.
- 11 Nakamura N, Hashimoto K, Matsunaga T. Immunoassay method for the determination of immunoglobulin G using bacterial magnetic particles. *Anal Chem* 1991; **63**: 268-272.
- 12 Grünberg K, Müller EC, Otto A, Reszka R, Linder D, Kube M *et al*. Biochemical and proteomic analysis of the magnetosome membrane in *Magnetospirillum gryphiswaldense*. *Appl Environ Microbiol* 2004; **70**: 1040-1050.
- 13 Xiang L, Bin W, Huali J, Wei J, Jiesheng T, Feng G *et al*. Bacterial magnetic particles (BMPs)-PEI as a novel and efficient non-viral gene delivery system. *J Gene Med* 2007; **9**: 679-690.
- 14 Zhang S, Zhang Y. Novel chemotactic-antigen DNA vaccine against cancer. *Future Oncol* 2008; **4**: 299-303.
- 15 Liu R, Zhou C, Wang D, Ma W, Lin C, Wang Y *et al*. Enhancement of DNA vaccine potency by sandwiching antigen-coding gene between secondary lymphoid tissue chemokine (SLC) and IgG Fc fragment genes. *Cancer Biol Ther* 2006; **5**: 427-434.
- 16 Bloquel C, Trollet C, Pradines E, Seguin J, Scherman D, Bureau MF. Optical imaging of luminescence for *in vivo* quantification of gene electrotransfer in mouse muscle and knee. *BMC Biotechnol* 2006; **6**: 16.
- 17 Zhang L, Conejo-Garcia JR, Katsaros D, Gimotty PA, Massobrio M, Regnani G *et al*. Intratumoral T cells, recurrence, and survival in epithelial ovarian cancer. *N Engl J Med* 2003; **348**: 203-213.
- 18 Bazylinski DA. Synthesis of the bacterial magnetosome: the making of a magnetic personality. *Int Microbiol* 1999; **2**: 71-80.
- 19 Matsunaga T. Applications of bacterial magnets. *Trends Biotechnol* 1991; **9**: 91-95.
- 20 Hopkin M. Magnet-making bacteria could target tumours. *Nature* 2004; e-pub ahead of print 8 September 2004; doi:10.1038/news040906-11.
- 21 Hergt R, Hiergeist R, Zeiberger M. Magnetic properties of bacterial magnetosomes as potential diagnostic and therapeutic tools. *J Magnet Magnet Mater* 2005; **293**: 80-86.
- 22 Han L, Zhang A, Wang H, Pu P, Jiang X, Kang C *et al*. Tat-BMPs-PAMAM conjugates enhance therapeutic effect of small interference RNA on U251 glioma cells *in vitro* and *in vivo*. *Hum Gene Ther* 2010; **21**: 417-426.
- 23 Yang NS, Burkholder J, Roberts B, Martinell B, McCabe D. *In vivo* and *in vitro* gene transfer to mammalian somatic cells by particle bombardment. *Proc Natl Acad Sci USA* 1990; **87**: 9568-9572.
- 24 Nagira M, Imai T, Hieshima K, Kusuda J, Ridanpaa M, Takagi S *et al*. Molecular cloning of a novel human CC chemokine secondary lymphoid-tissue chemokine that is a potent chemoattractant for lymphocytes and mapped to chromosome 9p13. *J Biol Chem* 1997; **272**: 19518-19524.
- 25 Kirk CJ, Hartigan-O'Connor D, Nickoloff BJ, Chamberlain JS, Giedlin M, Aukerman L *et al*. T cell-dependent antitumor immunity mediated by secondary lymphoid tissue chemokine: augmentation of dendritic cell-based immunotherapy. *Cancer Res* 2001; **61**: 2062-2070.
- 26 Sharma S, Stolina M, Luo J, Strieter RM, Burdick M, Zhu LX *et al*. Secondary lymphoid tissue chemokine mediates T cell-dependent antitumor responses *in vivo*. *J Immunol* 2000; **164**: 4558-4563.
- 27 Tolba KA, Bowers WJ, Muller J, Houseknecht V, Giuliano RE, Federoff HJ *et al*. Herpes simplex virus (HSV) amplicon-mediated codelivery of secondary lymphoid tissue chemokine and CD40L results in augmented antitumor activity. *Cancer Res* 2002; **62**: 6545-6551.
- 28 Stoecklinger A, Grieshuber I, Scheibelhofer S, Weiss R, Ritter U, Kissenpfennig A *et al*. Epidermal langerhans cells are dispensable for humoral and cell-mediated immunity elicited by gene gun immunization. *J Immunol* 2007; **179**: 886-893.
- 29 Porgador A, Irvine KR, Iwasaki A, Barber BH, Restifo NP, Germain RN. Predominant role for directly transfected dendritic cells in antigen presentation to CD8+ T cells after gene gun immunization. *J Exp Med* 1998; **188**: 1075-1082.
- 30 Trimble C, Lin CT, Hung CF, Pai S, Juang J, He L *et al*. Comparison of the CD8+ T cell responses and antitumor effects generated by DNA vaccine administered through gene gun, biojector, and syringe. *Vaccine* 2003; **21**: 4036-4042.
- 31 Hirose H, Nakahara T, Zhang QM, Yonei S, Mikakoshi J. Static magnetic field with a strong magnetic field gradient (41.7 T/m) induces C-Jun expression in HL-60 cells. *In Vitro Cell Dev Biol* 2003; **39**: 348-352.
- 32 Coletti D, Teodori L. Static magnetic fields enhance skeletal muscle differentiation *in vitro* by improving myoblast alignment. *Cytometry A* 2007; **71**: 846-856.
- 33 Pacini S, Gulisano M. Effects of 0.2 T static magnetic field on human skin fibroblasts. *Cancer Detect Prevent* 2003; **27**: 327-332.
- 34 Euguchi Y, Ogiue-Ikeda M. Control of orientation of rat Schwann cells using an 8 T static magnetic field. *Neurosci Lett* 2003; **351**: 130-132.
- 35 Higashi T, Yamagishi A. Orientation of erythrocytes in a strong magnetic field. *Blood* 1993; **82**: 1328-1334.
- 36 Dini L, Abbro L. Bioeffects of moderate-intensity static magnetic fields on cell cultures. *Micron* 2005; **36**: 195-217.
- 37 Smith CA, de la Fuente J, Pelaz B, Furlani EP, Mullin M, Berry CC. The effect of static magnetic fields and tat peptides on cellular and nuclear uptake of magnetic nanoparticles. *Biomaterials* 2010; **31**: 4392-4400.
- 38 Sun J, Tang T, Duan J, Xu PX, Wang Z, Zhang Y *et al*. Biocompatibility of bacterial magnetosomes: acute toxicity, immunotoxicity and cytotoxicity. *Nanotoxicology* 2010; **4**: 271-283.



This work is licensed under the Creative Commons Attribution-NonCommercial-No Derivative Works 3.0 Unported License. To view a copy of this license, visit <http://creativecommons.org/licenses/by-nc-nd/3.0/>